

# New Measurements of the $D_s^+ \rightarrow \phi \mu^+ \nu$ Form Factor Ratios

J. M. Link<sup>a</sup> P. M. Yager<sup>a</sup> J. C. Anjos<sup>b</sup> I. Bediaga<sup>b</sup> C. Göbel<sup>b</sup>  
A. A. Machado<sup>b</sup> J. Magnin<sup>b</sup> A. Massafferri<sup>b</sup>  
J. M. de Miranda<sup>b</sup> I. M. Pepe<sup>b</sup> E. Polycarpo<sup>b</sup> A. C. dos Reis<sup>b</sup>  
S. Carrillo<sup>c</sup> E. Casimiro<sup>c</sup> E. Cuautle<sup>c</sup> A. Sánchez-Hernández<sup>c</sup>  
C. Uribe<sup>c</sup> F. Vázquez<sup>c</sup> L. Agostino<sup>d</sup> L. Cinquini<sup>d</sup>  
J. P. Cumalat<sup>d</sup> J. Jacobs<sup>d</sup> B. O'Reilly<sup>d</sup> I. Segoni<sup>d</sup> K. Stenson<sup>d</sup>  
J. N. Butler<sup>e</sup> H. W. K. Cheung<sup>e</sup> G. Chiodini<sup>e</sup> I. Gaines<sup>e</sup>  
P. H. Garbincius<sup>e</sup> L. A. Garren<sup>e</sup> E. Gottschalk<sup>e</sup> P. H. Kasper<sup>e</sup>  
A. E. Kreymer<sup>e</sup> R. Kutschke<sup>e</sup> M. Wang<sup>e</sup> L. Benussi<sup>f</sup>  
M. Bertani<sup>f</sup> S. Bianco<sup>f</sup> F. L. Fabbri<sup>f</sup> A. Zallo<sup>f</sup> M. Reyes<sup>g</sup>  
C. Cawfield<sup>h</sup> D. Y. Kim<sup>h</sup> A. Rahimi<sup>h</sup> J. Wiss<sup>h</sup> R. Gardner<sup>i</sup>  
Y. S. Chung<sup>j</sup> J. S. Kang<sup>j</sup> B. R. Ko<sup>j</sup> J. W. Kwak<sup>j</sup> K. B. Lee<sup>j</sup>  
K. Cho<sup>k</sup> H. Park<sup>k</sup> G. Alimonti<sup>l</sup> S. Barberis<sup>l</sup> M. Boschini<sup>l</sup>  
A. Cerutti<sup>l</sup> P. D'Angelo<sup>l</sup> M. DiCorato<sup>l</sup> P. Dini<sup>l</sup> L. Edera<sup>l</sup>  
S. Erba<sup>l</sup> M. Giammarchi<sup>l</sup> P. Inzani<sup>l</sup> F. Leveraro<sup>l</sup> S. Malvezzi<sup>l</sup>  
D. Menasce<sup>l</sup> M. Mezzadri<sup>l</sup> L. Moroni<sup>l</sup> D. Pedrini<sup>l</sup>  
C. Pontoglio<sup>l</sup> F. Prezl<sup>l</sup> M. Rovere<sup>l</sup> S. Sala<sup>l</sup>  
T. F. Davenport III<sup>m</sup> V. Arena<sup>n</sup> G. Boca<sup>n</sup> G. Bonomi<sup>n</sup>  
G. Gianini<sup>n</sup> G. Liguori<sup>n</sup> M. M. Merlo<sup>n</sup> D. Pantea<sup>n</sup>  
D. Lopes Pegna<sup>n</sup> S. P. Ratti<sup>n</sup> C. Riccardi<sup>n</sup> P. Vitulo<sup>n</sup>  
H. Hernandez<sup>o</sup> A. M. Lopez<sup>o</sup> H. Mendez<sup>o</sup> A. Paris<sup>o</sup>  
J. E. Ramirez<sup>o</sup> Y. Zhang<sup>o</sup> J. R. Wilson<sup>p</sup> T. Handler<sup>q</sup>  
R. Mitchell<sup>q</sup> D. Engh<sup>r</sup> M. Hosack<sup>r</sup> W. E. Johns<sup>r</sup> E. Luiggi<sup>r</sup>  
M. Nehring<sup>r</sup> P. D. Sheldon<sup>r</sup> E. W. Vaandering<sup>r</sup> M. Webster<sup>r</sup>  
M. Sheaff<sup>s</sup>

<sup>a</sup>University of California, Davis, CA 95616

<sup>b</sup>Centro Brasileiro de Pesquisas Físicas, Rio de Janeiro, RJ, Brasil

<sup>c</sup>CINVESTAV, 07000 México City, DF, Mexico

<sup>d</sup>University of Colorado, Boulder, CO 80309

<sup>e</sup>Fermi National Accelerator Laboratory, Batavia, IL 60510

<sup>f</sup>*Laboratori Nazionali di Frascati dell'INFN, Frascati, Italy I-00044*

<sup>g</sup>*University of Guanajuato, 37150 Leon, Guanajuato, Mexico*

<sup>h</sup>*University of Illinois, Urbana-Champaign, IL 61801*

<sup>i</sup>*Indiana University, Bloomington, IN 47405*

<sup>j</sup>*Korea University, Seoul, Korea 136-701*

<sup>k</sup>*Kyungpook National University, Taegu, Korea 702-701*

<sup>l</sup>*INFN and University of Milano, Milano, Italy*

<sup>m</sup>*University of North Carolina, Asheville, NC 28804*

<sup>n</sup>*Dipartimento di Fisica Nucleare e Teorica and INFN, Pavia, Italy*

<sup>o</sup>*University of Puerto Rico, Mayaguez, PR 00681*

<sup>p</sup>*University of South Carolina, Columbia, SC 29208*

<sup>q</sup>*University of Tennessee, Knoxville, TN 37996*

<sup>r</sup>*Vanderbilt University, Nashville, TN 37235*

<sup>s</sup>*University of Wisconsin, Madison, WI 53706*

See <http://www-focus.fnal.gov/authors.html> for additional author information

---

## Abstract

Using a large sample of  $D_s^+ \rightarrow \phi \mu^+ \nu$  decays collected by the FOCUS photo-production experiment at Fermilab, we present new measurements of two semi-leptonic form factor ratios:  $r_\nu$  and  $r_2$ . We find  $r_\nu = 1.549 \pm 0.250 \pm 0.148$  and  $r_2 = 0.713 \pm 0.202 \pm 0.284$ . These values are consistent with  $r_\nu$  and  $r_2$  form factors measured for the process  $D^+ \rightarrow \bar{K}^{*0} \ell^+ \nu_\ell$ .

---

# 1 Introduction

This paper provides new measurements of the parameters that describe  $D_s^+ \rightarrow \phi \mu^+ \nu$  decays. The  $D_s^+ \rightarrow \phi \mu^+ \nu$  decay amplitude is described [1] by four form factors with an assumed (pole form)  $q^2$  dependence. Following earlier experimental work [2–13], the  $D_s^+ \rightarrow \phi \mu^+ \nu$  amplitude is then described by ratios of form factors taken at  $q^2 = 0$ . The traditional set is:  $r_2$ ,  $r_3$ , and  $r_v$  which we define explicitly after Equation 1. According to flavor SU(3) symmetry, one expects that the form factor ratios describing  $D_s^+ \rightarrow \phi \mu^+ \nu$  should be close to those describing  $D^+ \rightarrow \bar{K}^{*0} \mu^+ \nu$  since the  $D_s^+$  only differs from the  $D^+$  through the replacement of a  $\bar{d}$  quark by a  $\bar{s}$  quark spectator. The existing lattice gauge calculations [14,15] predict that the form factor ratios describing  $D_s^+ \rightarrow \phi \ell^+ \nu_\ell$  should lie within 10% of those describing  $D^+ \rightarrow \bar{K}^{*0} \ell^+ \nu_\ell$ . Although the measured  $r_v$  form factors are quite consistent between  $D_s^+ \rightarrow \phi \ell^+ \nu_\ell$  and  $D^+ \rightarrow \bar{K}^{*0} \ell^+ \nu_\ell$ , there is presently a  $3.3 \sigma$  discrepancy between the  $r_2$  values measured for these two processes with the previously measured  $D_s^+ \rightarrow \phi \ell^+ \nu_\ell$  value being a factor of about 1.8 times larger than the  $r_2$  value measured for  $D^+ \rightarrow \bar{K}^{*0} \ell^+ \nu_\ell$  [7]. One quark model calculation [16] offers a possible explanation for the apparent inconsistency in the  $r_2$  values measured for  $D^+ \rightarrow \bar{K}^{*0} \ell^+ \nu_\ell$  and  $D_s^+ \rightarrow \phi \ell^+ \nu_\ell$ .

Five kinematic variables that uniquely describe  $D_s^+ \rightarrow K^+ K^- \mu^+ \nu$  decay are illustrated in Figure 1. These are the  $K^- K^+$  invariant mass ( $m_{K^+ K^-}$ ), the square of the  $\mu\nu$  mass ( $q^2$ ), and three decay angles: the angle between the  $K^+$  and the  $D_s^+$  direction in the  $K^- K^+$  rest frame ( $\theta_v$ ), the angle between the  $\nu$  and the  $D_s^+$  direction in the  $\mu\nu$  rest frame ( $\theta_\ell$ ), and the acoplanarity angle between the two decay planes ( $\chi$ ). These angular conventions on  $\theta_\ell$  and  $\theta_v$  apply to both the  $D_s^+$  and  $D_s^-$ . The sign of the acoplanarity angle is defined via a cross product expression of the form:  $(\vec{P}_\mu \times \vec{P}_\nu) \times (\vec{P}_{K^-} \times \vec{P}_{K^+}) \cdot \vec{P}_{K^- K^+}$  where all momentum vectors are in the  $D_s^+$  rest frame. Since this expression involves five momentum vectors, as one goes from  $D_s^+ \rightarrow D_s^-$  one must change  $\chi \rightarrow -\chi$  in Equation 1 to get the same squared amplitude for the  $D_s^+$  and  $D_s^-$  assuming  $CP$  symmetry since all five vectors reverse sign under  $CP$ .

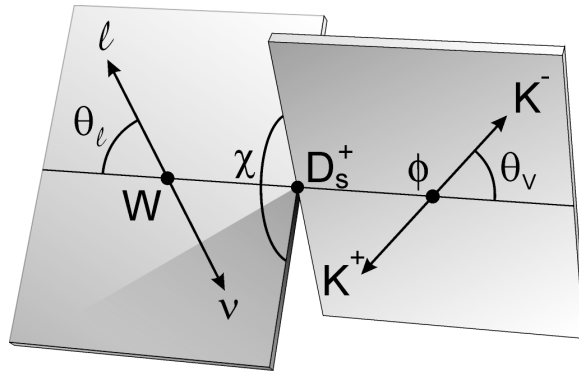


Fig. 1. Definition of kinematic variables.

Using the notation of [1], we write the decay distribution for  $D_s^+ \rightarrow \phi \mu^+ \nu$  in terms of the four helicity basis form factors:  $H_+$ ,  $H_0$ ,  $H_-$ ,  $H_t$ .

$$\frac{d^5\Gamma}{dm_{KK} dq^2 d\cos\theta_V d\cos\theta_\ell d\chi} \propto K(q^2 - m_l^2) \left\{ \left| \begin{array}{l} (1 + \cos\theta_\ell) \sin\theta_V e^{i\chi} B_\phi H_+ \\ - (1 - \cos\theta_\ell) \sin\theta_V e^{-i\chi} B_\phi H_- \\ - 2 \sin\theta_\ell (\cos\theta_V B_\phi + A e^{i\delta}) H_0 \end{array} \right|^2 \right. \\ \left. + \frac{m_\ell^2}{q^2} \left| \begin{array}{l} \sin\theta_\ell \sin\theta_V B_\phi (e^{i\chi} H_+ + e^{-i\chi} H_-) \\ + 2 \cos\theta_\ell (\cos\theta_V B_\phi + A e^{i\delta}) H_0 \\ + 2 (\cos\theta_V B_\phi + A e^{i\delta}) H_t \end{array} \right|^2 \right\} \quad (1)$$

where  $K$  is the momentum of the  $K^- K^+$  system in the rest frame of the  $D_s^+$ , and  $A e^{i\delta}$  is an  $s$ -wave amplitude which couples to the virtual  $W^+$ . The first term gives the squared amplitude for the  $\mu^+$  to be right-handed, while the (highly suppressed) second term gives the squared amplitude for it to be left-handed. The helicity basis form factors are given by:

$$\begin{aligned} H_\pm(q^2) &= (M_D + m_{KK}) A_1(q^2) \mp 2 \frac{M_D K}{M_D + m_{KK}} V(q^2) \\ H_0(q^2) &= \frac{1}{2m_{KK}\sqrt{q^2}} \left[ (M_D^2 - m_{KK}^2 - q^2)(M_D + m_{KK}) A_1(q^2) - 4 \frac{M_D^2 K^2}{M_D + m_{KK}} A_2(q^2) \right] \\ H_t(q^2) &= \frac{M_D K}{m_{KK}\sqrt{q^2}} \left[ (M_D + m_{KK}) A_1(q^2) - \frac{(M_D^2 - m_{KK}^2 + q^2)}{M_D + m_{KK}} A_2(q^2) + \frac{2q^2}{M_D + m_{KK}} A_3(q^2) \right] \end{aligned} \quad (2)$$

The vector and axial form factors are generally parameterized by a pole dominance form:

$$A_i(q^2) = \frac{A_i(0)}{1 - q^2/M_A^2} \quad V(q^2) = \frac{V(0)}{1 - q^2/M_V^2}$$

where we use nominal (spectroscopic) pole masses of  $M_A = 2.5 \text{ GeV}/c^2$  and  $M_V = 2.1 \text{ GeV}/c^2$ . The  $B_\phi$  denotes the Breit-Wigner amplitude describing the

$\phi$  resonance:<sup>1</sup>

$$B_\phi = \frac{\sqrt{m_0}\Gamma\left(\frac{P^*}{P_0^*}\right)}{m_{KK}^2 - m_0^2 + im_0\Gamma\left(\frac{P^*}{P_0^*}\right)^3}$$

Equation 1 includes a possible  $s$ -wave amplitude ( $Ae^{i\delta}$ ) coupling to the virtual  $W^+$  with the same  $q^2$  dependence as that of the  $H_0$  (or  $H_t$ ) form factor. Evidence for such an  $s$ -wave amplitude term for the decay  $D^+ \rightarrow K^-\pi^+\mu^+\nu$  was presented in Reference [3]. An explicit search was made for  $s$ -wave amplitude interference with the process  $D_s^+ \rightarrow \phi\mu^+\nu$  and no evidence for this interference was seen. We were able to limit the  $s$ -wave contribution to be less than 5% of the maximum of the  $\phi$  Breit-Wigner peak in the  $H_0$  piece of Equation 1 at the 90% confidence level. The results presented here will therefore assume  $A = 0$  in Equation 1. Under these assumptions, the decay squared amplitude is then parameterized by the  $r_v \equiv V(0)/A_1(0)$ ,  $r_2 \equiv A_2(0)/A_1(0)$ ,  $r_3 \equiv A_3(0)/A_1(0)$  form factor ratios describing the  $D_s^+ \rightarrow \phi\mu^+\nu$  amplitude.

Throughout this paper, unless explicitly stated otherwise, the charge conjugate is also implied when a decay mode of a specific charge is stated.

## 2 Experimental and analysis details

The data for this paper were collected in the Wideband photoproduction experiment FOCUS during the Fermilab 1996–1997 fixed-target run. In FOCUS, a forward multi-particle spectrometer is used to measure the interactions of high energy photons on a segmented BeO target. The FOCUS detector is a large aperture, fixed-target spectrometer with excellent vertexing and particle identification. Most of the FOCUS experiment and analysis techniques have been described previously [3,17–19,21]. Our analysis cuts were chosen to give reasonably uniform acceptance over the five kinematic decay variables, while maintaining a strong rejection of backgrounds. To suppress background from the re-interaction of particles in the target region which can mimic a decay vertex, we required that the charm secondary vertex was located at least three standard deviations outside of all solid material including our target and target microstrip system. We will refer to this as the "out-of-material" cut.

---

<sup>1</sup> We are using a  $p$ -wave Breit-Wigner form with a width proportional to the cube of the kaon momentum in the kaon-kaon rest frame ( $P^*$ ) over the value of this momentum when the kaon-kaon mass equals the resonant mass ( $P_0^*$ ). The squared modulus of our Breit-Wigner form will have an effective  $P^{*3}$  dependence in the numerator as well. Two powers  $P^*$  come explicitly from the  $P^*$  in the numerator of the amplitude and one power arises from the 4 body phase space.

To isolate the  $D_s^+ \rightarrow \phi \mu^+ \nu$  topology, we required that candidate muon, pion, and kaon tracks appeared in a secondary vertex with a confidence level exceeding 1%. The muon track, when extrapolated to the shielded muon arrays, was required to match muon hits with a confidence level exceeding 5%. The kaon was required to have a Čerenkov light pattern more consistent with that of a kaon than that of a pion by 1 unit of log likelihood [19]. To further reduce non-charm background we required that our primary vertex consisted of at least two charged tracks. To further reduce muon misidentification, a muon candidate was allowed to have at most one missing hit in the 6 planes comprising our inner muon system and an energy exceeding 10 GeV. In order to suppress muons from pions and kaons decaying within our apparatus, we required that each muon candidate had a confidence level exceeding 1% to the hypothesis that it had a consistent trajectory through our two analysis magnets.

Non-charm and random combinatoric backgrounds were reduced by requiring both a detachment between the vertex containing the  $K^- K^+ \mu^+$  and the primary production vertex of at least 5 standard deviations.

Possible background from  $D^+ \rightarrow K^- K^+ \pi^+$ , where a pion is misidentified as a muon, was reduced by treating the muon as a pion and requiring the reconstructed  $KK\pi$  mass be less than  $1.8 \text{ GeV}/c^2$ . The  $m_{K^+K^-}$  distribution for our  $D_s^+ \rightarrow K^+ K^- \mu^+ \nu$  candidates is shown in Figure 2.

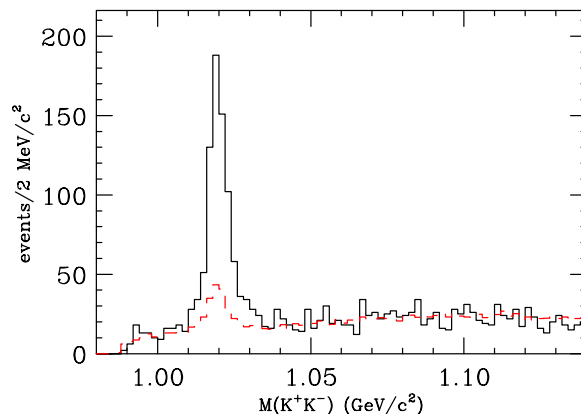


Fig. 2. The  $m_{K^+K^-}$  mass distribution for events satisfying our signal selection cuts. The solid histogram is our data. The dashed histogram is distribution for the cbar background Monte Carlo. The cbar background Monte Carlo is normalized to the same number of events in the sideband region  $1.040 \text{ GeV}/c^2 < m_{K^+K^-} < 1.14 \text{ GeV}/c^2$ .

It was important to test the fidelity of the simulation with respect to reproducing the resolution of those kinematic variables which depend on the neutrino momentum. To do this, we studied fully-reconstructed  $D^0 \rightarrow K^- \pi^+ \pi^+ \pi^-$  decays where, as a test, one of the pions was reconstructed using our line-of-flight technique. We then compared its reconstructed momentum to its original, magnetic reconstruction in order to obtain an “observed” resolution function that was well matched by our simulation.

### 3 Fitting Technique

The  $r_v$  and  $r_2$  form factors were fit to the probability density function described by four fitted kinematic variables ( $q^2$ ,  $\cos\theta_V$ ,  $\cos\theta_\ell$ , and  $\chi$ ) for decays in the mass range  $1.010 < m_{K+K^-} < 1.030$  GeV/ $c^2$  using the squared amplitude described by Eqn. 1.<sup>2</sup>

We use a variant of the continuous fitting technique developed by the E691 Collaboration [20] for fitting decay squared amplitudes where several of the kinematic variables have very poor resolution such as the four variables that rely on reconstructed neutrino kinematics.

The fit which determines the  $r_v$  and  $r_2$  form factor ratios minimizes the sum of  $w = -2 \ln I$  where  $I$  is the normalized decay squared amplitude at each event. The squared amplitude at each event is estimated by the squared intensity of Monte Carlo events that lie within a small window of each of the four (reconstructed) kinematic variables of the given event.<sup>3</sup> Some care is needed in choosing a reasonable size of the windows since too small a window will result in fluctuations due to finite Monte Carlo statistics, and too large a window will create a bias in the result. Our principal tool in deciding a reasonable window was to check for biases and fluctuations outside of reported statistical errors using a Monte Carlo simulation that included charm backgrounds with  $r_v$  and  $r_2$  values very close to the result reported here. Variations in the final results due to the window choice were included in the estimate of the systematic error.

Two Monte Carlos were employed: a  $D_s^+ \rightarrow \phi \mu^+ \nu$  signal Monte Carlo that was generated flat in the four fitted kinematic variables ( $q^2$ ,  $\cos\theta_V$ ,  $\cos\theta_\ell$ , and  $\chi$ ) and then weighted by the squared amplitude appropriate for the  $r_v$  and  $r_2$  on each fit iteration and a background Monte Carlo which simulated all known charm decays (apart from the  $D_s^+ \rightarrow \phi \mu^+ \nu$  signal) as well as our misidentification levels. The squared amplitude about each event is an appropriate average of the signal Monte Carlo and the background Monte Carlo. The averaging depended on the background fraction determined by matching the number of events in the  $\phi$  sideband region  $1.040 < m_{K+K^-} < 1.14$  GeV/ $c^2$  in the background Monte Carlo to the sideband level observed in the data.

Our fit was to the  $r_v$  and  $r_2$  form factor ratios with  $r_3$  and the possible  $s$ -wave amplitude set to zero. The  $r_3$  form factor is the ratio of the  $A_3(0)/A_1(0)$  form factors defined in the  $H_t$  expression of Eqn. (2). We decided not to fit for the

---

<sup>2</sup> Only two parameters are required since  $r_3$  was assumed to be zero as was the  $s$ -wave amplitude. The background level was fixed using the  $\phi$  sideband and signal yield was then normalized to the number of remaining events in the mass interval from  $1.010 < m_{K+K^-} < 1.030$  GeV/ $c^2$ .

<sup>3</sup> A Monte Carlo event had to lie within 0.08 to each event in both  $\cos\theta_V$  and  $\cos\theta_\ell$ , within 0.18 radians in  $\chi$ , and within 0.8 GeV<sup>2</sup>/ $c^2$  in  $q^2$ .

$r_3$  form factor ratio since our anticipated  $r_3$  error given our sample size would be too large to be meaningful.<sup>4</sup>

Figure 3 compares the data and model for projections of  $\cos\theta_V$ ,  $\cos\theta_\ell$ ,  $\chi$  and  $q^2/q_{\max}^2$ . Most of these distributions follow the predicted values reasonably well. A slight discrepancy is evident in the low  $q^2/q_{\max}^2$  projection (below  $q^2/q_{\max}^2 < 0.2$ ). A stronger effect was observed in Reference [2] possibly owing to our much larger yield in the  $D^+ \rightarrow K^-\pi^+\mu^+\nu$  final state.

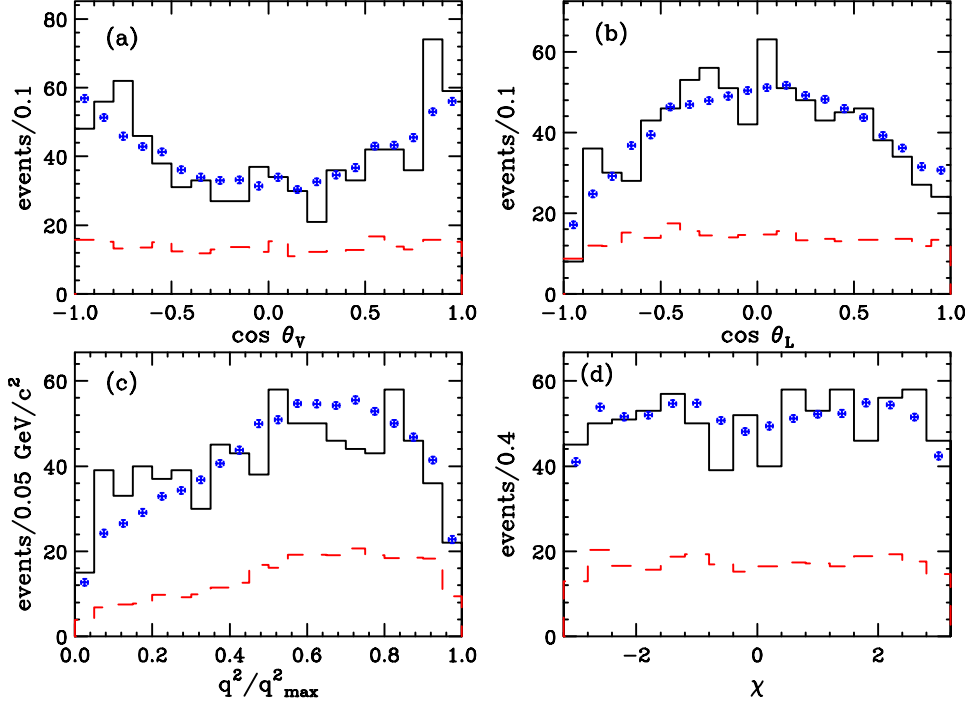


Fig. 3. Distributions for a)  $\cos\theta_V$  (b)  $\cos\theta_\ell$  (c)  $q^2/q_{\max}^2$  and (d)  $\chi$ . The data are given by the upper histogram. The model (crosses with flats) includes the signal computed with the fitted form factor ratios plus the sideband normalized cbar background. The lower histogram (dashed) shows the projections of the cbar background.

Figure 4 compares the  $\cos\theta_V$  and  $\cos\theta_\ell$  distribution between the data and our Monte Carlo model for events at high and low  $q^2$ . As  $q^2 \rightarrow q_{\max}^2$  one expects an isotropic distribution in both  $\cos\theta_V$  and  $\cos\theta_\ell$  since all three helicity basis form factors become equal. The data presented in Figure 4 match this expectation relatively well.

<sup>4</sup> Reference [6] reports on a first measurement of  $r_3$  for the reaction  $D^+ \rightarrow \bar{K}^{*0}\ell^+\nu_\ell$  of  $r_3 = 0.04 \pm 0.33 \pm 0.29$ .

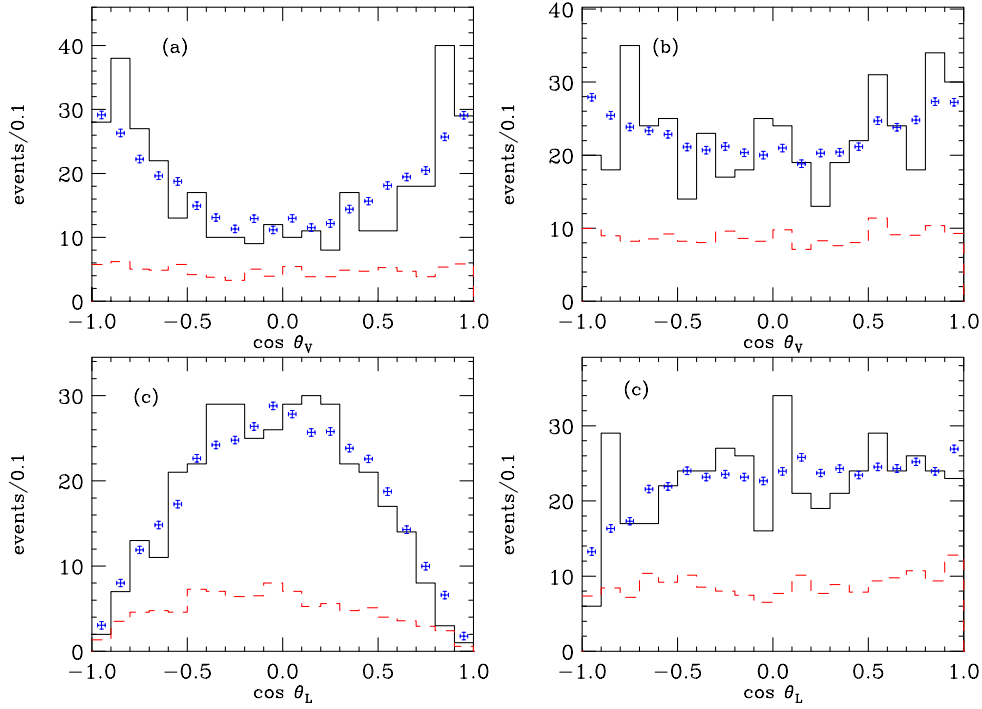


Fig. 4.  $\cos \theta_V$  and  $\cos \theta_\ell$  projections in different intervals of  $q^2/q^2_{\max}$ . (a) The  $\cos \theta_V$  distribution for  $q^2/q^2_{\max} < 0.5$  (b) The  $\cos \theta_V$  distribution for  $q^2/q^2_{\max} > 0.5$  (c) The  $\cos \theta_\ell$  distribution for  $q^2/q^2_{\max} < 0.5$  (d) The  $\cos \theta_\ell$  distribution for  $q^2/q^2_{\max} > 0.5$ . The data are given by the upper histogram. The model (crosses with flats) includes the signal computed with the fitted form factor ratios plus the sideband normalized  $c\bar{c}$  background. The lower histogram (dashed) shows the projections of the  $c\bar{c}$  background.

#### 4 Form Factor Ratio Systematic Errors

Three basic approaches were used to determine the systematic error on the form factor ratios. In the first approach, we measured the stability of the  $r_v$  and  $r_2$  measurements with respect to variations in analysis cuts designed to suppress backgrounds. We believe the cut variant systematic provides an estimate of systematic effects due to potential non-charm backgrounds as well as checks of the fidelity of our Monte Carlo in reproducing acceptance variation. These included removing the (1) out-of-material cut, (2) increasing our detachment cut from 5 standard deviations to 10 standard deviations, (3) increasing our Cerenkov likelihood cut to distinguish kaons from pions from 1 unit to 2 units of likelihood, and (4) requiring that the secondary vertex was well isolated.<sup>5</sup> Sixteen cut sets ( $2^4$ ) where each of the 4 modified cuts is applied in turn were considered. The loosest cut selection had 2496 events in the signal region ( $1.010 < m_{K^+K^-} < 1.030 \text{ GeV}/c^2$ ) and a background fraction of 54.2%. The tightest cut selection had 326 events in the signal region and had

<sup>5</sup> The vertex isolation cut required that no other track (not in the primary vertex) could be associated with the  $K^+K^-\mu^+$  vertex with a confidence level exceeding 0.1 %.

a background fraction of 19.5%. The "cut variation" systematic presented in Table 1 was computed from the variance of  $r_v$  and  $r_2$  estimates obtained in fits over the sixteen cut selections.

In the second approach, we split our sample according to a variety of criteria deemed relevant to our acceptance, production, and decay models and estimated a systematic based on the consistency of the form factor ratio measurements among the split samples. These included computing separate form factors for particles versus antiparticles, comparing the values obtained over the full data set to values obtained from the subset (2/3) of the data in which the target silicon [21] was operational, and comparing the form factors measured for events with  $m_{K+K^-}$  above versus below the  $\phi(1019)$  pole. A split sample systematic error was added in quadrature to the existing statistical error to make the split sample estimates consistent to within  $1\sigma$  if necessary. No split sample systematic error was required for any of the splits considered.

In the third approach we checked the stability of the branching fraction as we varied specific parameters in our Monte Carlo model and fitting procedure. The three parameter variation systematic errors were determined from the difference change in the form factor ratios by (1) Varying the level of the charm background (by  $\pm 25\%$  over the value determined by the  $\phi$ -sideband) (2) Decreasing volume of the kinematic windows used to associate Monte Carlo events with data points in the computation of the fitting squared amplitude by a factor of three and (3) Varying  $r_3$  by plus or minus twice the (statistical and systematic) error reported by E791 [6] for the reaction  $D^+ \rightarrow \bar{K}^{*0} \ell^+ \nu_\ell$  ( $r_3 = 0.04 \pm 0.33 \pm 0.29$ ).

Combining all of non-zero systematic error estimates in Table 1 in quadrature, we find  $r_v = 1.549 \pm 0.250 \pm 0.148$  and  $r_2 = 0.713 \pm 0.202 \pm 0.284$ .

Table 1  
Contributions to the systematic error

Source	$r_v$	$r_2$
cut variation	0.145	0.266
particle versus antiparticle	0	0
$m_{K+K^-} < 1.019 \text{ GeV}/c^2$ versus $m_{K+K^-} > 1.019 \text{ GeV}/c^2$	0	0
late runs versus early runs	0	0
neighborhood size	0.030	0.095
background variation	0.011	0.004
$r_3$ variation	0.006	0.036
<b>total systematic</b>	<b>0.148</b>	<b>0.284</b>

## 5 Summary

In Table 2 we compare our results to other experiments. Our weighted average of all the experimental results is  $r_v = 1.678 \pm 0.213$  and  $r_2 = 1.31 \pm 0.197$  where systematic errors have been included. We obtain a confidence level of 44.3% that all 5 experiments have a consistent  $r_v$  and a confidence level of 23.4 % that all  $r_2$  measurements are consistent. Figure 5 is a graphical representation of Table 2.

Table 2

Measurements of the  $D_s^+ \rightarrow \phi \mu^+ \nu$  form factor ratios

Group	$r_v$	$r_2$
This work	$1.549 \pm 0.250 \pm 0.148$	$0.713 \pm 0.202 \pm 0.284$
E791[7]	$2.27 \pm 0.35 \pm 0.22$	$1.570 \pm 0.250 \pm 0.190$
CLEO[8]	$0.9 \pm 0.6 \pm 0.3$	$1.400 \pm 0.500 \pm 0.300$
E653[12]	$2.3 \pm 1.0 \pm 0.4$	$2.100 \pm 0.550 \pm 0.200$
E687[10]	$1.8 \pm 0.9 \pm 0.2$	$1.100 \pm 0.800 \pm 0.100$

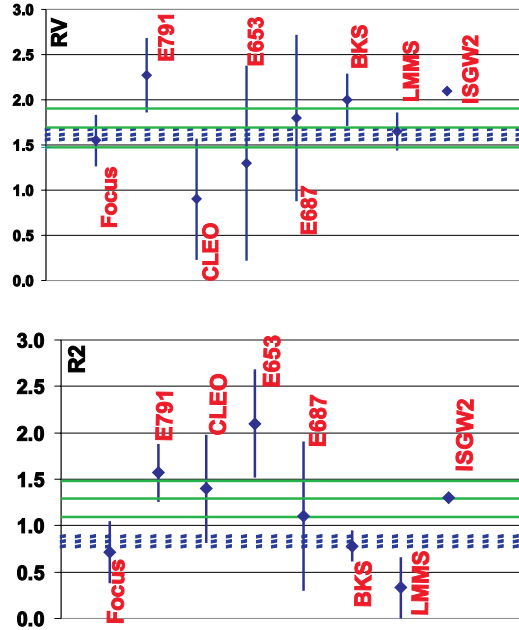


Fig. 5. Comparison to previous data and calculations of the  $D_s^+ \rightarrow \phi \mu^+ \nu$  form factors. The three solid lines represent the weighted average of the world's experimental data for  $D_s^+ \rightarrow \phi \mu^+ \nu$  and  $\pm 1 \sigma$ . The three dashed lines represent the weighted average of the world's experimental data on  $D^+ \rightarrow \bar{K}^{*0} \mu^+ \nu$  and  $\pm 1 \sigma$ . Our average for  $D^+ \rightarrow \bar{K}^{*0} \mu^+ \nu$  was  $r_v = 1.62 \pm .055$  and  $r_2 = 0.830 \pm 0.054$ . The references for the points marked Focus, E791, CLEO, and E687 are given in Table 2. The three calculations are labeled BES [14], LMMS [15], and ISGW2 [16].

Our measured  $r_v$  and  $r_2$  values for  $D_s^+ \rightarrow \phi \mu^+ \nu$  are very consistent with our measured  $r_v$  and  $r_2$  values for  $D^+ \rightarrow \overline{K}^{*0} \mu^+ \nu$  [2] and therefore consistent with the theoretical expectation that the form factors for the two processes should be very similar.

## 6 Acknowledgments

We wish to acknowledge the assistance of the staffs of Fermi National Accelerator Laboratory, the INFN of Italy, and the physics departments of the collaborating institutions. This research was supported in part by the U. S. National Science Foundation, the U. S. Department of Energy, the Italian Istituto Nazionale di Fisica Nucleare and Ministero dell'Università e della Ricerca Scientifica e Tecnologica, the Brazilian Conselho Nacional de Desenvolvimento Científico e Tecnológico, CONACyT-México, the Korean Ministry of Education, and the Korean Science and Engineering Foundation.

## References

- [1] J.G. Korner and G.A. Schuler, Z. Phys. C 46 (1990) 93.
- [2] FOCUS Collab., J.M. Link et al., Phys. Lett. B 544 (2002) 89.
- [3] FOCUS Collab., J.M. Link et al., Phys. Lett. B 535 (2002) 43.
- [4] BEATRICE Collab., M. Adamovich et al., Eur. Phys. J. C 6 (1999) 35.
- [5] E791 Collab., E. M. Aitala et al., Phys. Rev. Lett. 80 (1998) 1393.
- [6] E791 Collab., E. M. Aitala et al., Phys. Lett. B 440 (1998) 435.
- [7] E791 Collab. E.M. Aitala et al., Phys. Lett. B 450 (1999) 294.
- [8] CLEO Collab. P. Avery et al., Phys. Lett. B 337 (1994) 405.
- [9] E687 Collab., P.L. Frabetti et al., Phys. Lett. B 307 (1993) 262.
- [10] E687 Collab. P. L. Frabetti et al., Phys. Lett. B 328 (1994) 187.
- [11] E653 Collab., K. Kodama et al., Phys. Lett. B 274 (1992) 246.
- [12] E653 Collab. K. Kodama et al., Phys. Lett. B 309 (1993) 483.
- [13] E691 Collab., J. C. Anjos et al., Phys. Rev. Lett. 65 (1990) 2630.
- [14] C. W. Benard, A. X. El-Khadra, and A. Soni, Phys. Rev. D45 (1992) 869.
- [15] V. Lubicz, G. Martinelli, M. S. McCarthy, and C. T. Sachrajda, Phys. Lett. B 274 (1992) 415.

- [16] D. Scora and N. Isgur, *Phys. Rev. D* 52 (1995) 2783.
- [17] E687 Collab., P. L. Frabetti et al., *Nucl. Instrum. Methods A* 320 (1992) 519.
- [18] FOCUS Collab., J. M. Link et al., *Phys. Lett. B* 485 (2000) 62.
- [19] FOCUS Collab., J. M. Link et al., *Nucl. Instrum. Methods A* 484 (2002) 270.
- [20] D.M. Schmidt, R.J. Morrison, and M.S. Witherell, *Nucl. Instrum. Methods. A* 328 (1993) 547.
- [21] FOCUS Collab., J. M. Link et al., *Nucl. Instrum. Methods A* 516 (2003) 364.